Defense Technical Information Center
Compilation Part Notice

ADP012808

TITLE: Influence of Localization on the Optical Nonlinearities Induced by Exciton-Exciton Interaction in Semiconductor Nanostructures

DISTRIBUTION: Approved for public release, distribution unlimited
Availability: Hard copy only.

This paper is part of the following report:

TITLE: Nanostructures: Physics and Technology International Symposium [6th] held in St. Petersburg, Russia on June 22-26, 1998 Proceedings

To order the complete compilation report, use: ADA406591

The component part is provided here to allow users access to individually authored sections of proceedings, annals, symposia, etc. However, the component should be considered within the context of the overall compilation report and not as a stand-alone technical report.

The following component part numbers comprise the compilation report:
ADP012712 thru ADP012852

Influence of localization on the optical nonlinearities induced by exciton-exciton interaction in semiconductor nanostructures

Jørn M. Hvam and Wolfgang W. Langbein

Mikroelektronik Centret, The Technical University of Denmark, Building 345 east, DK–2800 Lyngby, Denmark

Abstract. The signature of exciton-exciton interaction in the four-wave mixing response at the fundamental excitonic resonance is investigated as a function of the localization strength in GaAs single and multiple quantum wells. The four-wave mixing is found to be dominated by signals induced by exciton-exciton interaction. For co-polarization of the incident pulses, excitation-induced dephasing (EID) is dominating the signal generation, while for cross-linear polarized excitation, the signal is generated from bound and unbound biexciton transitions. The relative strength of the EID compared to phase-space filling shows a maximum for localization energies comparable to the homogeneous broadening. The biexciton binding energy increases for localization energies comparable to or larger than the biexciton binding, while the biexciton continuum edge shifts to energies above the exciton resonance. Simultaneously, the binding energy gets inhomogeneously broadened, and the oscillator strength of the biexciton continuum is reduced by the quantization of the excitonic states in the localization potential.

1 Introduction

The role of exciton-exciton interactions in the nonlinear coherent response of semi-conductor nanostructures is discussed intensively in recent literature [1, 2, 3, 4]. The important role of the excitation-induced dephasing [5, 6] has been pointed out. The description of the nonlinear optical response by few-level models including bound and unbound biexciton states [4, 7, 8], as introduced by Bott *et al.* [1], has been compared with the solutions of the Semiconductor Bloch Equations beyond the Hartree-Fock approximation [9, 10, 11]. For localized systems, the theoretical description using few-level models is the only one presently feasible. In the inhomogeneously broadened case, the excitonic as well as the biexcitonic four-wave mixing (FWM) signal is a photon echo [12, 13, 14]. The biexcitonic FWM shows a fast, non-exponential decay in delay time due to the inhomogeneous broadening of the biexciton binding energy [15]. Also, the average binding energy of the biexciton is enhanced by the localization [16, 17, 18, 19].

In this paper we give an overview over the influence of exciton localization on the EID and the biexcitonic spectrum. In the absence of localization, the biexciton spectrum consists of one bound and a continuum of unbound states [11]. The onset of the continuum is at twice the exciton energy at zero center-of-mass motion ($\mathbf{K} = 0$). In FWM experiments, mainly the bound state and the onset of the continuum is active due to the exciton $\mathbf{K} = 0$ components of the respective biexciton states. The localized biexciton case can be compared to previous investigations on three-dimensionally confined quantum dot systems [20]. Here, one observes unbound (excited) biexciton states above the two-exciton energy [21, 22] additionally to the bound biexciton state [23]. In structures with statistical disorder, the random potential leads to localized zero-dimensional states

[19]. Consequently, localization should similarly lead to a quantization of the biexciton continuum.

2 Samples and experiment

We use a set of GaAs quantum well (QW) samples with well thicknesses between 4 nm and 25 nm, embedded in $Al_{0.3}Ga_{0.7}As$ barriers. They are grown by molecular beam epitaxy on nominally undoped (100) GaAs substrates, and are single QW (SQW) or 10–15 period multiple QW (MQW) structures. We perform polarization-dependent transient FWM in reflection or transmission geometry with spectrally resolved, time-integrated detection. The incident pulses in the directions $\mathbf{k}_1$ and $\mathbf{k}_2$ with τ_{12} temporal separation were generated by a self–mode–locked Ti:sapphire laser at 76 MHz repetition rate. The pulses are chirp compensated and spectrally shaped to a duration between 100 fs and 3 ps. The pulse spectra were adjusted to overlap the heavy-hole 1s exciton and biexciton transition, while excluding higher resonances. The FWM signal in the $2\mathbf{k}_2 - \mathbf{k}_1$ direction is selected spatially by pinholes and detected spectrally resolved by a combination of a spectrometer and an optical multichannel analyzer. The excited exciton densities are $1-5 \times 10^9$/cm^2. All experiments are performed at 5 K lattice temperature.

3 Results and discussion

The polarization selection rules in FWM can be used to single out transitions from the ground state of the crystal $|0\rangle$ to one of the optically active exciton states X, or transitions from an X state to a biexciton state (bound XX or unbound XX*). The involved selection rules are derived from a five-level optical Bloch equation model displayed in either a circular-polarized or linear-polarized exciton basis [1, 14], as indicated in Fig. 1a,b.

Using co-circular polarized $\mathbf{k}_1$ and $\mathbf{k}_2$ pulses $(\sigma^+\sigma^+)$, no biexcitonic transitions can be excited (Fig. 1a). The FWM signal is (σ^+) polarized, and originates from the $|0\rangle$-X transition. The corresponding FWM spectra (Fig. 1c) show accordingly a single resonance with an inhomogeneous broadening Γ_X that is increasing with decreasing well width.

In the nearly homogeneously broadened 25 nm SQW (homogeneous broadening $2\gamma_X = 2\hbar/T_2 \approx 140$ μeV, $\Gamma_X \approx 30$ μeV,), the FWM signal is a free polarization decay (FPD) for $|\tau_{12}| < \hbar/\Gamma_X$. On the other hand, in the inhomogeneously broadened 10 nm and 4 nm QWs the FWM signal is a photon echo (PE), and is suppressed for $\tau_{12} < -\hbar/\Gamma_X$ [12]. We have confirmed the PE nature of the FWM signal by time-resolved FWM, and we do not observe the change from FPD to PE with delay time for cross-linear polarization as previously reported [24, 25].

The $(\sigma^+\sigma^+\sigma^+)$ signal can be in general due to excitation-induced dephasing (EID) [5, 6], Local field effects (LFE) [26], and phase-space filling (PSF). For the 25 nm sample, the signal does no show a step-like increase from negative to positive delay (Fig. 1c), indicating that PSF, that is only active for positive delay, is not dominant. EID and LFE are distinguished by the beating with the two-photon coherence (TPC) at negative delay (Fig. 2a). The beating observed for $(\rightarrow\rightarrow\rightarrow)$ polarization is largely suppressed for $(\rightarrow\uparrow\rightarrow)$ polarization, thus excluding the polarization-independent LFE, and leaving EID as the dominant $(\sigma^+\sigma^+\sigma^+)$ and $(\rightarrow\rightarrow\rightarrow)$ FWM mechanism. The weak beating for $(\rightarrow\uparrow\rightarrow)$ polarization is due to a small LFE contribution.
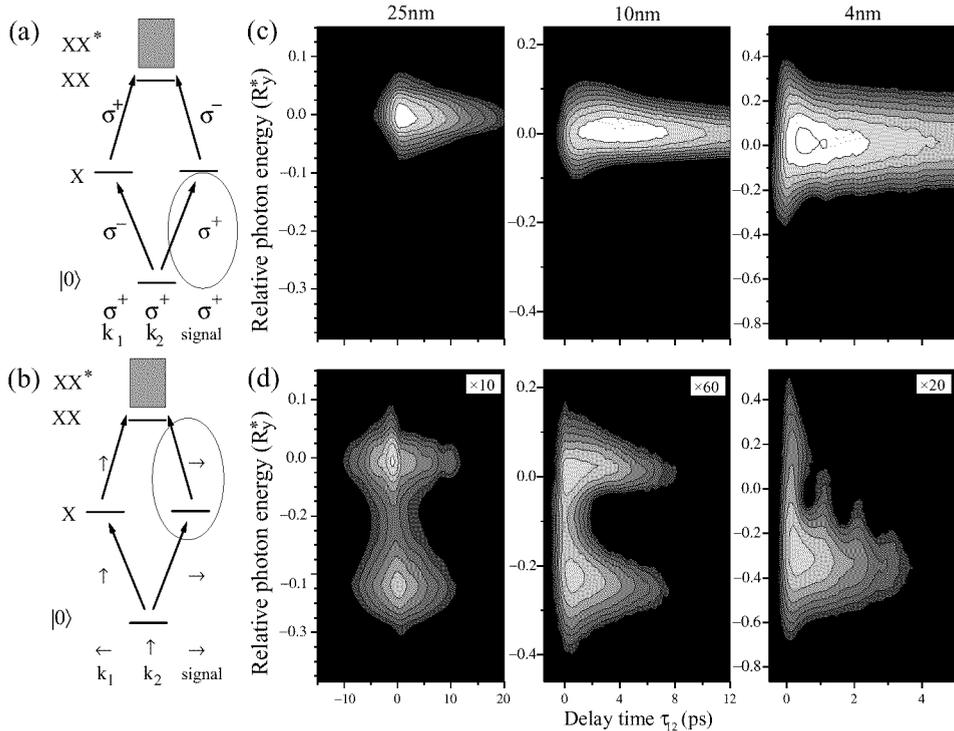
Fig 1. (a)-(b) Schematic representation of the considered five-level system and its optical transitions for a circular (a) or a linear (b) polarized exciton basis. The transitions emitting the FWM signal $P^{(3)}$ in $2\mathbf{k_2} - \mathbf{k_1}$ direction are encircled. (c)-(d) Spectrally resolved FWM intensity as a function of τ_{12} for co-circular ($\sigma^+\sigma^+\sigma^+$) (c) and cross-linear ($\rightarrow\uparrow\rightarrow$) (d) polarization of the excitation and detection. Data for the 25 nm and 10 nm SQWs, and the 4 nm MQW are given. The logarithmic contour scale covers 3 orders of magnitude. The intensity scalings between the two polarization configurations are given. The photon energy is offset with the respective $|0\rangle$-X transition energy E_X, and scaled with the exciton binding energy R_y^*. The excitation spectra cover the displayed photon energy range.

The EID changes character in an inhomogeneous system. If the EID is dependent only on the macroscopic density, it should vanish due to destructive interference within the inhomogeneous distribution and no PE is generated [6]. On the other hand, if the EID is dependent only on the microscopic densities, the EID generates a PE intensity with a quadratic delay-time dependence relative to the PSF signal.

The observed signal intensity ratio between ($\rightarrow\rightarrow\rightarrow$) and ($\rightarrow\uparrow\rightarrow$) polarization increases for a small inhomogeneous broadening (Fig. 2b) and always keeps larger than 10. This shows that EID is the dominant FWM mechanism also in the inhomogeneously broadened case. However, the delay-time dependence of the time-integrated ($\rightarrow\rightarrow\rightarrow$) FWM signal at the exciton transition matches closely the expected response of the PSF in the inhomogeneous case, and does not show an additional τ_{12}^2 dependence, as demonstrated by the fitted curves according to the PSF mechanism [12] (Fig. 2a). The
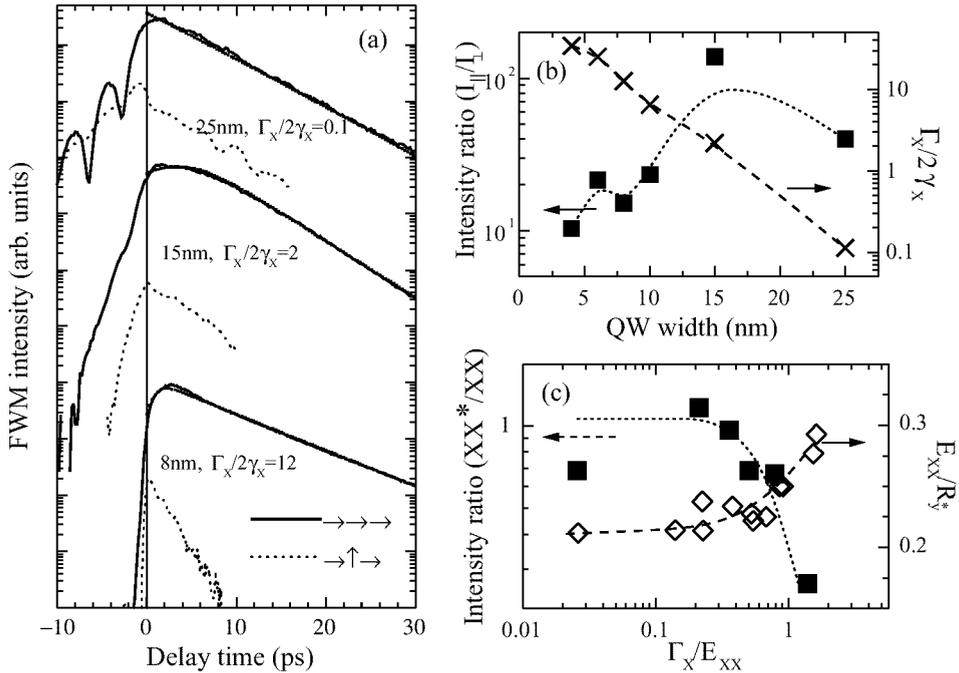
Fig 2. (a) Time-integrated FWM intensity at the $0\rangle$-X transition energy using $(\rightarrow\rightarrow\rightarrow)$ (solid line) and $(\rightarrow\uparrow\rightarrow)$ (dotted line) polarization for SQW widths as indicated. The data are vertically offset for each SQW width. Dots: fitted behaviour for PSF in presence of inhomogeneous broadening. The ratio between inhomogeneous Γ_X and homogeneous $2\gamma_X$ broadenings is given. (b) Signal intensity ratio between $(\rightarrow\rightarrow\rightarrow)$ and $(\rightarrow\uparrow\rightarrow)$ polarization at zero delay time (squares), and inhomogeneous to homogeneous broadening ratio $\Gamma_X/2\gamma_X$ (crosses) as a function of well width. The lines are guides for the eye. (c) biexciton to exciton binding energy ratio E_{XX}/R_y^* (diamonds) and ratio between the X-XX* and X-XX FWM intensity at a $\tau_{12} = h/E_{XX}$ (squares) as a function of the biexcitonic localization Γ_X/E_{XX}. The lines are guides for the eye.

EID in inhomogeneously broadened systems is thus not described simply by neither of the above pictures.

A possible description is given by an EID dephasing rate $\gamma'(\Delta E)$, which is scaling with the inverse energy separation ΔE^{-1} between two interacting subsystems within the inhomogeneous distribution. This results in an EID delay-time dependence similar to PSF. Direct measurements of $\gamma'(\Delta E)$ by FWM with an additional, spectrally narrow prepump [27, 28] are in agreement with this model. For large inhomogeneous broadening, the EID contribution decreases (Fig. 2b). This might be due to the smaller exciton density of states D(E) or a smaller wavefunction overlap. A detailed analysis of the FWM processes in dependence of the inhomogeneous broadening will be published elsewhere [29, 28].

Using cross-linear polarized $\mathbf{k}_1$ and $\mathbf{k}_2$ pulses $(\rightarrow\uparrow)$, the FWM signal originates only from the X-XX and X-XX* transitions. It is $(\rightarrow)$ polarized, and due to PSF. We want to emphasis here that the X-XX* transition is different from the $|0\rangle$-X transition, and

thus shows in general different oscillator strengths and dephasing times, even though it can have the same transition energy. Previously, the observed different dephasing times for co and cross-linear polarization have been explained by disorder induced coupling [30] or EID [5, 27].

The measured $(\rightarrow\uparrow\rightarrow)$ FWM signal (Fig. 1d) consists of two distinct resonances, namely the X-XX and X-XX* transition, with the relative energies E_{XX} and E_{XX^*} to the $|0\rangle$-X energy E_X. The total signal intensity is reduced by one to two orders of magnitude compared to $(\sigma^+\sigma^+\sigma^+)$ polarization due to the missing EID contribution and due to the distribution of the exciton oscillator strength into two spectrally separated transitions (assuming here that the oscillator strength of the exciton is not changed significantly by the exciton-exciton interaction).

In the 25nm SQW, the signal decay for $\tau_{12} < 0$ shows the dephasing of the XX $(T_2 = 7\,\text{ps})$ and XX* $(T_2 = 6\,\text{ps})$ states. An exciton dephasing with $T_2 = 9\,\text{ps}$ is deduced for $\tau_{12} > 0$, in agreement with the value found for $(\sigma^+\sigma^+\sigma^+)$ polarization. The biexciton continuum edge transition X-XX* coincides with the energy of the $|0\rangle$-X transition $(E_{XX^*} = 0)$. The respective homogeneous broadenings $2\gamma_{XX^*} = 220\,\mu\text{eV} > 2\gamma_{XX} = 180\,\mu\text{eV} > 2\gamma_X = 140\,\mu\text{eV}$ show that the biexcitonic states have a higher scattering cross-section. However, the scattering rate is not simply doubled, indicating that the spin-scattering of the excitons forming the biexciton is reduced.

In the inhomogeneous broadened case with $\Gamma_X < E_{XX}$ (as for the 10 nm SQW), the two biexciton resonances are still spectrally separated. Note that here the energy of the X-XX* transition is higher than the $|0\rangle$-X transition, i.e. $E_{XX^*} > 0$, showing that these transitions are in fact different. The biexcitonic FWM signals decay significantly faster than the exciton signal for $(\sigma^+\sigma^+\sigma^+)$ polarization, which shows T_2 times larger than 8 ps for all investigated samples. This is due to the inhomogeneous broadenings $\Gamma_{XX(XX^*)}$ of the biexcitonic energy shifts $E_{XX(XX^*)}$, introduced by the disorder [15], as can be explained as follows. After the arrival of $\mathbf{k}_1$, the first-order polarization is propagating at the $|0\rangle$-X frequency ω_X. After the arrival of $\mathbf{k}_2$, the corresponding third-order polarization is propagating on the X-XX(XX*) frequency $\omega_{XX(XX^*)}$ until the emission of the PE. Since the frequencies of the two transitions $(\omega_X, \omega_{XX(XX^*)})$ are not perfectly correlated [12, 31] (i.e. there are no $\alpha > 0$, and β for which $\hbar\omega_{XX(XX^*)} = \alpha\hbar\omega_X + \beta$ holds), the rephasing of the PE is incomplete, and the signal decay is determined by $\Gamma_{XX(XX^*)}$ (assuming that the PE width is small compared to the dephasing times i.e. $\gamma_X, \gamma_{XX(XX^*)} \ll \Gamma_X$).

The $(\rightarrow\uparrow\rightarrow)$ FWM signal again changes character for $\Gamma_X \geq E_{XX}$ (like in the 4 nm MQW). The quantum beat between the X-XX and X-XX* transition now present in delay time because the PE duration is smaller than the beat period [14, 31]. Additionally, the X-XX* signal shows a reduced strength compared to the nearly free case, and the energy shift E_{XX^*} of the unbound biexciton is clearly visible.

The FWM decay rate for both biexcitonic transitions is strongly increasing with increasing Γ_X (see Fig. 1d and 2a). This shows that $\Gamma_{XX(XX^*)}$ are increasing (assuming that $\gamma_{XX(XX^*)} \ll \Gamma_{XX(XX^*)}$, which is reasonable since $\gamma_X \ll \Gamma_{XX}$). The energy shifts $E_{XX(XX^*)}$ of the biexcitonic transitions for various QW widths can be extracted from the FWM spectra for $(\rightarrow\uparrow\rightarrow)$ polarization (see Fig. 1d). The respective Γ_X gives rise to the increasing spectral width of the transitions with decreasing well width. An increasing E_{XX}/R_y^* with increasing localization is observed (see Fig. 2c). This results from a quenching of the zero-point kinetic energy of the exciton-exciton motion in the biexciton

[16, 17]. Simultaneously, the repulsion energy E_{XX^*} increases by approximately the same amount. This is due to the finite splitting between the ground and excited state of the exciton center-of-mass motion in the localization potential. The oscillator strength of the X-XX* transition is decreasing relative to the X-XX transition in the strong localization case $\Gamma_X \geq E_{XX}$. We attribute this to the lower $\mathbf{K} = 0$ component of the excited localized exciton state.

4 Conclusions

In conclusion, we have shown that the optically active biexcitonic spectrum in quantum wells is strongly influenced by a localization potential, which is inevitably introduced by the interfaces. With increasing degree of localization, the binding energy of the bound state increases, and the unbound biexciton state (biexcitonic continuum) is quantized to higher energies. This also creates an inhomogeneous broadening of the bound and unbound biexcitons energies relative to the corresponding exciton energy. As a result, the biexcitonic four-wave mixing signal shows a fast decay in delay time due to the incomplete rephasing of the photon echo. This explains previously observed strong polarization dependence of the FWM dynamics at the excitonic transitions as due to biexcitonic interactions.

References

 [1] K. Bott *et al.*, *Phys. Rev. B* **48** 17418 (1993).
 [2] K. H. Pantke *et al.*, *Phys. Rev. B* **47** 2413 (1993).
 [3] K. Ferrio and D. Steel, *Phys. Rev. B* **54** R5231 (1996).
 [4] A. Paul, J. Bolger, A. Smirl, and J. Pellegrino, *J. Opt. Soc. Am. B* **13** 1016 (1996).
 [5] Y. Z. Hu *et al.*, *Phys. Rev. B* **49** 14382 (1994).
 [6] H. Wang *et al.*, *Phys. Rev. B* **49** R1551 (1994).
 [7] E. Mayer *et al.*, *Phys. Rev. B* **51** 10909 (1995).
 [8] G. Finkelstein, S. Bar-Ad, O. Carmel, and I. Bar-Joseph, *Phys. Rev. B* **47** 12964 (1993).
 [9] W. Schäfer *et al.*, *Phys. Rev. B* **53** 16429 (1996).
[10] V. Axt, G. Bartels, and A. Stahl, *Phys. Rev. Lett.* **76** 2543 (1996).
[11] T. Östreich, K. Schönhammer, and L. Sham, *Phys. Rev. Lett.* **74** 4698 (1995).
[12] J. Erland *et al.*, *Phys. Rev. B* **50** 15047 (1994).
[13] T. Saiki, M. Kuwata-Gonokami, T. Matsusue, and H. Sakaki, *Phys. Rev. B* **49** 7817 (1994).
[14] T. F. Albrecht *et al.*, *Phys. Rev. B* **54** 4436 (1996).
[15] W. Langbein *et al.*, *Phys. Rev. B* **55** R7383 (1997).
[16] W. Langbein and J. M. Hvam, *Phys. stat. sol. (b)* **206** 111 (1998).
[17] W. Langbein and J. M. Hvam, unpublished.
[18] W. Langbein, P. Borri, and J. Hvam, in *RDPS 98, Trends in Optics and Photonics Series*, edited by D. Citrin (Optical Society of America, Washington D.C., 1998), Vol. 18.
[19] K. Brunner *et al.*, *Phys. Rev. Lett.* **73** 1138 (1994).
[20] Y. Z. Hu, M. Lindberg, and S. W. Koch, *Phys. Rev. B* **42** 1713 (1990).
[21] U. Woggon *et al.*, *Phys. Rev. B* **47** 3684 (1993).
[22] M. Ikezawa, Y. Masumoto, T. Takagahara, and S. V. Nair, *Phys. Rev. Lett.* **79** 3522 (1997).

[23] Y. Z. Hu *et al.*, *Phys. Rev. Lett.* **64** 1805 (1990).

[24] M. D. Webb, S. T. Cundiff, and D. G. Steel, *Phys. Rev. Lett.* **66** 934 (1991).

[25] H. Schneider and K. Ploog, *Phys. Rev. B* **49** 17050 (1994).

[26] M. Wegener, D. Chemla, S. Schmitt-Rink, and W. Schäfer, *Phys. Rev. A* **42** 5675 (1990).

[27] P. Borri *et al.*, *Phys. stat. sol. (a)* **164** 61 (1997).

[28] W. Langbein, P. Borri, and J. M. Hvam, unpublished.

[29] W. Langbein, P. Borri, and J. M. Hvam, *IQEC 1998 OSA Technical Digest Series* (Optical Society of America, Washington D.C., 1998).

[30] D. Bennhardt *et al.*, *Phys. Rev. B* **47** 13485 (1993).

[31] S. T. Cundiff, *Phys. Rev. A* **49** 3114 (1994).